International Journal of Heat and Fluid Flow 30 (2009) 1218–1229

Contents lists available at ScienceDirect

International Journal of Heat and Fluid Flow

journal homepage: www.elsevier.com/locate/ijhff

# A 3D study on the effect of gate location on the cooling of polymer by injection molding

Hamdy Hassan *, Nicolas Regnier, Guy Defaye

*TREFLE Laboratory, Bordeaux 1, UMR 8508, Site ENSCPB, 16 av Pey Berland, 33607 Pessac Cedex, France*

ARTICLE INFO

*Article history:*
Received 6 February 2009
Received in revised form 13 May 2009
Accepted 15 June 2009
Available online 7 July 2009

*Keywords:*
Gate location
Injection molding
Polymer
Cooling
Solidification

ABSTRACT

Injection molding is one of the most widely used plastic part processing. The quality of the injection molded part is a function of plastic material, part geometry, mold structure and process conditions. Gate location is among the most critical factors in achieving dimensionally accurate parts and high productivity of the molding process. To investigate the effect of the gate location on the cooling of polymer by injection molding, a full three dimensional time-dependent analysis is carried out for a mold with cuboids-shape cavity having two different thicknesses. The cooling of the polymer material is carried out by cooling water flowing inside six horizontal circular channels. Three gate locations are assumed, normal to the cavity surface, normal to the small thickness of the cavity, and normal to the large thickness of the cavity. A numerical model by finite volume is used for the solution of the physical model. A validation of the numerical model is presented. The results show that the gate location normal to the small thickness of the cavity achieves the minimum time required to completely solidify the product and minimum solidification of the product during the filling stage. They also indicate that the temperature distribution through the output product is greatly affected by the position of the injection gate location.



## 1. Introduction

Plastic industry is one of the world's fastest growing industries, ranked as one of the few billion-dollar industries. Almost every product that is used in daily life involves the usage of plastic and most of these products can be produced by plastic injection molding method. Injection molding is one of the most important plastics manufacturing process for producing plastic parts of complex shape of highest precision at high efficiency and low cost (Min, 2003). The plastic injection molding process is a cyclic process where polymer is injected into a mold cavity, and solidifies to form a plastic part. There are three significant stages in each cycle. The cavity is filled with melt hot polymer at an injection temperature and after the cavity is filled, additional polymer melt is packed into the cavity at a higher pressure to compensate the expected shrinkage as the polymer solidifies (filling and post-filling stage). It is followed by taking away the heat of the polymer to the cooling channels until the product completely solidifies (cooling stage), finally the solidified part is ejected (ejection stage) (Tang et al., 2006). The placement of a gate in an injection mold is one of the most important variables of the total mold design. The quality of the molded part is greatly affected by the gate location, because it influences the manner that the plastic flows into the mold cavity. Therefore, different gate locations introduce inhomogeneity in orientation, density, pressure, and temperature distribution and accordingly introduce different value and distribution of warpage (Li et al., 2007). Gate location is in relation with polymer capability, part shape and dimension, mold structure and molding conditions. Hence, it has great effect on the polymer molecule orientation and warpage of injection molding part after cooling. Irrational gate location would lead to short shot, warpage, shrinkage, weld and meld lines, air traps and other quality defects (Huang et al., 2008). Kima et al. (2003) presented a design guideline of gate location by investigating resin flow patterns obtained by numerical analysis for several different gate positions of a simple strip with a hinge. The analysis of the simple strip part showed that the resin at the hinge did not flow until the other side of the part was filled. Kang et al. (2000) showed that the more effective method for enhancing the flow is to use multiple injection gates. In this method, all the injection gates are opened simultaneously. Since each gate fills a smaller volume than the gate in a single gate injection molding, the filling time can be reduced. The problem in the multiple gate system is the entrapment of air bubbles when the flow fronts from two or more gates merge. Lee and Kim (1996) developed an automated selection method of gate location, in which a set of initial gate locations were proposed by a designer and then the optimal gate was located by the adjacent node evaluation method. The conclusion to a great

* Corresponding author. Tel.: +33 0540006348; fax: +33 0540002731.
*E-mail addresses:* hassan@enscpb.fr, hamdyaboali@yahoo.com (H. Hassan).

0142-727X/$ - see front matter © 2009 Elsevier Inc. All rights reserved.
doi:10.1016/j.ijheatfluidflow.2009.06.005

**Nomenclatures**

| | |
|---|---|
| $B$ | polymer material constant (Pa s) |
| $C$ | fractional volume function |
| $C_P$ | specific heat (J kg$^{-1}$ K$^{-1}$) |
| $f_s$ | solid fraction |
| $g$ | acceleration gravity (m$^{-1}$ s$^{-2}$) |
| $K$ | permeability |
| $L$ | latent heat of fusion (J kg$^{-1}$) |
| $N$ | normal condition |
| $n$ | power index |
| $p$ | pressure (Pa) |
| $Q$ | flow rate (m$^3$ s$^{-1}$) |
| $S_c$ | Source term (W m$^{-3}$) |
| $T$ | temperature (K) |
| $t$ | time (s) |
| $T_b$ | polymer material constant (K) |
| $V$ | velocity (m s$^{-1}$) |

*Greek symbols*

| | |
|---|---|
| $\alpha$ | thermal diffusivity (m$^2$ s$^{-1}$) |
| $\tau^*$ | critical stress level (Pa) |
| $\tau$ | viscous shear stress tensor (Pa) |
| $\mu$ | dynamic viscosity (Pa s) |
| $\eta$ | shear rate viscosity (Pa s) |
| $\beta$ | polymer material constant (Pa$^{-1}$) |
| $\rho$ | density (kg m$^{-3}$) |
| $\lambda$ | thermal conductivity (W m$^{-1}$ K$^{-1}$) |
| $\dot{\gamma}$ | equivalent shear rate (s$^{-1}$) |
| $\eta_o$ | zero shear rate (Pa s) |
| $\Gamma$ | entry region to the mold cavity |
| $\Gamma_4$ | entry region to the cooling channels |

*Subscripts*

| | |
|---|---|
| 1, 2, 3 | gate positions |
| $a$ | air |
| $B$ | sensitivity parameter |
| $c$ | cooling channels |
| $f$ | melting |
| $l$ | liquid |
| $o$ | intial |
| $p$ | polymer |
| $s$ | solid |
| $\infty$ | ambient condition |

extent depends much on the human designer's intuition, because the first step of the method is based on the designer's proposition. So the result is to a large extent limited to the designer's experience. Zhai et al. (2005) presented a two gate location optimization of one molding cavity by an efficient search method based on pressure gradient (PGSS), and subsequently positioned weld lines to the desired locations. Zhai et al. (2006) indicated that for large-volume part, multiple gates are needed to shorten the maximum flow path, with a corresponding decrease in injection pressure. This method is promising for design of gates and runners for a single cavity with multiple gates. Kima et al. (2003) used an empirical search method to predict the optimal gate location of injection molding. In their work the gate location scope is initiated by the practical experience of the mold designer. Haddad et al. (2008) tried to determine the ideal gate location and its effect on the product property by using the experiences of the previous engineers and make the analysis by using the computer software. They did the analysis based on the flow analysis of the plastic material through different gate locations.

In this paper, three dimensional study is presented for the effect of the gate location on the solidification and temperature distribution during the cooling of polymer material (polystyrene) by injection molding. The polymer material has the form of cuboids with two different thicknesses. The cooling process is carried out by cooling water flowing inside six cooling channels. Three positions for the gate location are assumed, normal to the cavity surface, normal to the large thickness of the cavity and normal to the small thickness of the cavity as shown in Fig. 1 (dimensions, mm). A finite volume method is used for the simulation of the physical model. A validation of the numerical model is presented.

## 2. Mathematical model

The mathematical equations governing the physical model must take into considerations: the injection of the polystyrene material into the mold cavity, the solidification of the polymer material during the cooling process, the flow of the cooling fluid inside the cooling channels, etc.

During the filling, cooling, solidification and ejection of the product, the following assumptions are introduced for the mathematical model.

The polystyrene material and cooling water flowing inside the cooling channels are considered non compressible fluids.

The sprue and runners system is omitted from the model because of the simplicity of the model.

The physical and thermal properties ($\rho$, $\lambda$, $C_P$) of the polystyrene, mold, and cooling water are considered constant during the simulation.

Generally the mathematical equations governing the physical model are the mass, momentum and energy equations:

$$\nabla \cdot V = 0 \tag{1}$$

$$\rho\left[\frac{\partial V}{\partial t} + (V\nabla)\cdot V\right] = -\nabla P + \rho g + \nabla\cdot(\tau) \tag{2}$$

$$\rho C_P\left[\frac{\partial T}{\partial t} + (V\nabla)\cdot T\right] = \nabla(\lambda\nabla T) + \eta\dot{\gamma}^2 \tag{3}$$

In addition to the conservation laws, the polymer viscosity is function of the shear rate, temperature, and pressure. In modeling the viscosity, a cross type equation is used (Chiang et al., 1991).

$$\eta = \frac{\eta_o(T,p)}{1+\left[\eta_o(T,p)\frac{\dot{\gamma}}{\tau^*}\right]^{1-n}} \tag{4}$$

where $\tau^*$ is a critical stress level at which $\eta$ is in transition between the Newtonian limits.

An Arrhenius law with temperature sensitivity and exponential pressure dependence is used for $\eta_o$ and is represented by Chiang et al. (1991).

$$\eta_o(T,p) = B\exp\left(\frac{T_b}{T}\right)\exp(\beta p) \tag{5}$$

The rheological model constants of the selected polystyrene material are listed in Table 1 (Chiang et al., 1991; Alexandra, 2004).

The momentum equation is closely coupled with the viscosity constitutive relation. The following simple linear averages are adopted in this work to approximate the viscosity and density at the interface between the polymer melt and the air (Vincent, 1999)

$$\begin{cases} \rho = \rho_a + (\rho_p - \rho_a)C \\ \mu = \mu_a + (\mu_p - \mu_a)C \end{cases} \tag{6}$$

The fractional phase function $C$ is defined as follows.

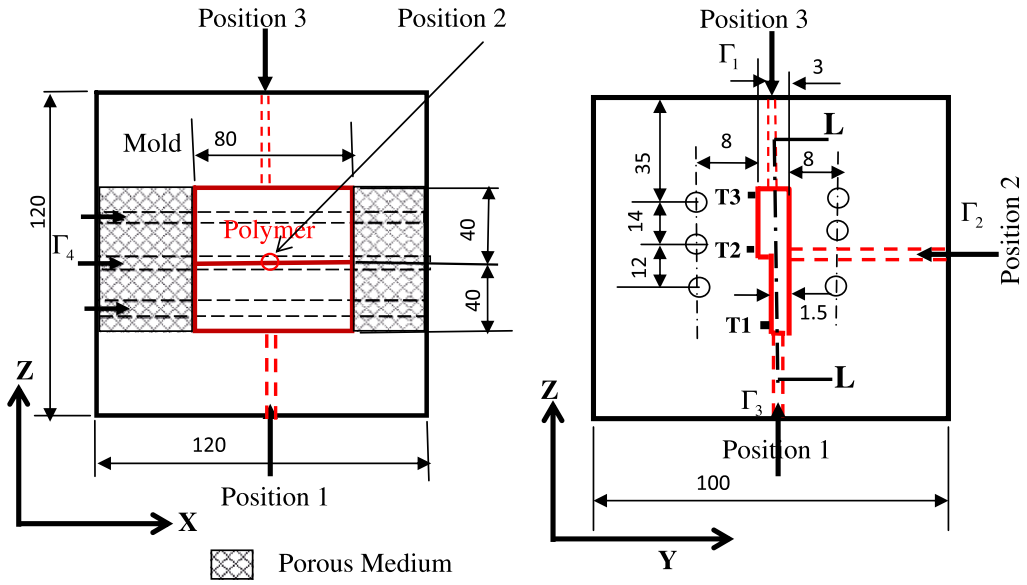


**Fig. 1.** Mold structure with polymer cavity, cooling channels and different gate locations (dimension, mm).

**Table 1**
The rheological model constants.

| Material constant | PS |
|---|---|
| $n$ | $2.7 \times 10^{-01}$ |
| $\tau^*$ (Pa) | $2.31 \times 10^{04}$ |
| $B$ (Pa s) | $3.04 \times 10^{-9}$ |
| $T_b$ (K) | 13,300 |
| $ß$ ($Pa^{-1}$) | $3.5 \times 10^{-8}$ |

$$C = \begin{cases} 1 & \text{for the point inside polymer} \\ 0 & \text{for the point inside air} \end{cases} \tag{7}$$

Then the interface is located within the cells where $0 < C < 1$. The phase function is governed by a transport equation.

$$\frac{\partial C}{\partial t} + V \cdot \nabla C = 0 \tag{8}$$

This equation determines the movement of interface position.

In order to take into account the solidification, a source term is added to the energy equation corresponding to heat absorption or heat release (Le, 2003) through phase change process. The energy equation in this case is represented as follows:

$$\rho C_P \left[\frac{\partial T}{\partial t} + (V\nabla)\cdot T\right] = \nabla \cdot (\lambda \nabla T) + \eta\dot{\gamma}^2 + S_c \tag{9}$$

where the source term $S_c$ is represented by:

$$S_c = \rho L \frac{\partial f_s}{\partial t} \tag{10}$$

where $f_s(T) = 0$ at $T \succ T_f$ (fully liquid region) $0 \prec f_s \prec 1$ at $T = T_f$ (isothermal phase change region) and, $f_s(T) = 1$ at $T \prec T_f$ (fully solid region). This technique is applied on fixed nodes and it enables to use the implicit method in the solution, and by using this technique the solidification could be applied at a defined temperature. This technique was already validated in previous studies by Le (2003) and Vincent and Arquis (2000).

This system of equations with the following boundary conditions is used to determine the different solution parameters (pressure, velocity, temperature, etc.) of the physical model.

*At the inlet to the mold cavity:*

During filling stage, constant polymer flow rate and constant inlet temperature are considered for the polymer material.

$$Q = Q_p \quad \text{and} \quad T = T_p \text{ on } \Gamma_1 \text{ or } \Gamma_2 \text{ or } \Gamma_3 \tag{11}$$

During cooling stage, zero inlet velocity and adiabatic boundary condition are assumed at the inlet.

At the inlet to the cooling channels: constant flow rate and constant inlet temperature are assumed for the cooling water.

$$Q = Q_c \quad \text{and} \quad T = T_\infty \text{ on } \Gamma_4 \tag{12}$$

At mold side walls, adiabatic boundary conditions are assumed.

## 3. Numerical solution

The numerical solution of the mathematical model governing the behavior of the physical system is computed by finite volume method. The equations are solved by an implicit treatment for the different terms of the equations system. The solution of the discretized equations are solved by an iterative algorithm of Augmented Lagrangian. In our numerical solution, we use the concept of a unique system of equations which is solved in the whole numerical domain (one fluid model). For this system, penalization terms are added to the general system of equations (Arquis and Caltagirone, 1984) to take into account different boundary conditions and solid mold zone. Using this technique of unique system makes it simple, suitable for different physical models.

### 3.1. Solid obstacles

To deal with solid mold within the numerical domain, it is possible to use multi-grid domains, but it is often very much simpler to implement the Brinkman theory (Arquis and Caltagirone, 1984). The numerical domain is then considered as a unique porous medium. The permeability coefficient $K$ defines the capability of a porous medium to let pass the fluid more or less freely through it. If this permeability coefficient is greater ($K \to +\infty$), the medium is equivalent to a fluid. If ($K \to 0$), then the medium is equivalent to a solid. A real porous medium is modeled with intermediate values of $K$. It is possible to model moving rigid boundaries or complex geometries. To take this coefficient $K$ into account in our system of equations, an extra term, called Darcy term $\frac{\mu}{K}V$ (Arquis and

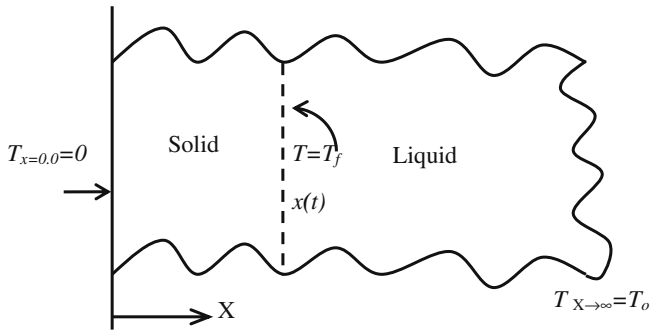


**Fig. 2.** Solidification of semi infinite solid.

**Table 2**
Properties of selected material and numerical parameters.

| Property | Unit | Liquid | Solid |
|---|---|---|---|
| Density, $\rho$ | kg m$^{-3}$ | 998 | 998 |
| Specific heat, $C_P$ | J kg$^{-1}$ K$^{-1}$ | 4182 | 2037 |
| Thermal conductivity, $\lambda$ | W m$^{-1}$ K$^{-1}$ | 0.6 | 2.2 |
| Latent heat, $L$ | J kg$^{-1}$ | 333,000 | |
| $T_o$ | °C | 140 | |
| $\Delta x$ | m | $8\times10^{-4}$ | |
| $\Delta t$ | s | 0.2 | |
| $T_f$ | °C | 0.0 | |
| Number of grids | | $125\times8$ | |

Caltagirone, 1984) is added to the momentum Eq. (2), and then the momentum equation becomes

$$\rho\left[\frac{\partial V}{\partial t}+(V\nabla)\cdot V\right]=-\nabla P+\rho g+\nabla\cdot(\tau)-\frac{\mu}{K}V \tag{13}$$

Practically, values of $K = 10^{+20}$ and $K = 10^{-20}$ are imposed to obtain liquid and solid medium, respectively.

### 3.2. Boundary conditions

To deal with the boundary conditions within the numerical domain, the method consists in writing a generalized boundary condition as a surface flux (Vincent and Caltagirone, 2000).

$$-\left(\frac{\partial V}{\partial N}\right)_{surface}=B_V(V-V_\infty) \tag{14}$$

where $B_V$ is a matrix. It has to be noted that it is a vectorial formulation and then involves the three Cartesian components of the velocity vector $V$. The boundary condition is directly taken into account in Eq. (14) then, we have the following equation:

$$\rho\left[\frac{\partial V}{\partial t}+(V\nabla)\cdot V\right]+B_V(V-V_\infty)=-\nabla P+\rho g+\nabla\cdot(\tau)-\frac{\mu}{K}V \tag{15}$$

Thanks to this penalization term, we can then impose a velocity in the numerical domain or on a lateral boundary. For $B_V = 0$, Neumann boundary conditions are modeled where $\left(\frac{\partial V}{\partial N}\right)=0$. Some coefficients are chosen as $B_V = +\infty$ to ensure Dirichlet boundary conditions imposed at the mesh grid points of the boundary.

The same procedure is used to impose the boundary condition in case of the Energy equation. The quantity $B_T(T-T_\infty)$ is introduced in Eq. (9) and then the following equation for the energy is solved (Vincent and Caltagirone, 2000):

$$\rho C_P\left[\frac{\partial T}{\partial t}+(V\nabla)\cdot T\right]+B_T(T-T_\infty)=\nabla\cdot(\lambda\nabla T)+\eta\dot{\gamma}^2+S_c \tag{16}$$

where

$$B_T=0:\ \text{Neumann condition}\left(\frac{\partial T}{\partial N}=0\right) \tag{17}$$

$$B_T\to\infty:\ \text{Dirichiet condition}\ (T=T_\infty) \tag{18}$$

Further details on the numerical model are available in Angot (1989) and Khadra et al. (1994). To validate this numerical model, we use an analytical solution known in cases of filling a square cavity, and a solidification of a semi infinite medium.

### 3.3. Validation

#### 3.3.1. Transient solidification of semi infinite medium

Solidification modeling is validated by using the analytical case of the solidification of semi infinite medium (Feidt, 1990). It is initially at liquid state and at a temperature $T_o$ greater than the solidification temperature $T_f$ and that the surface $x = 0.0$ is proposed at temperature less than $T_f$ as shown in Fig. 2.

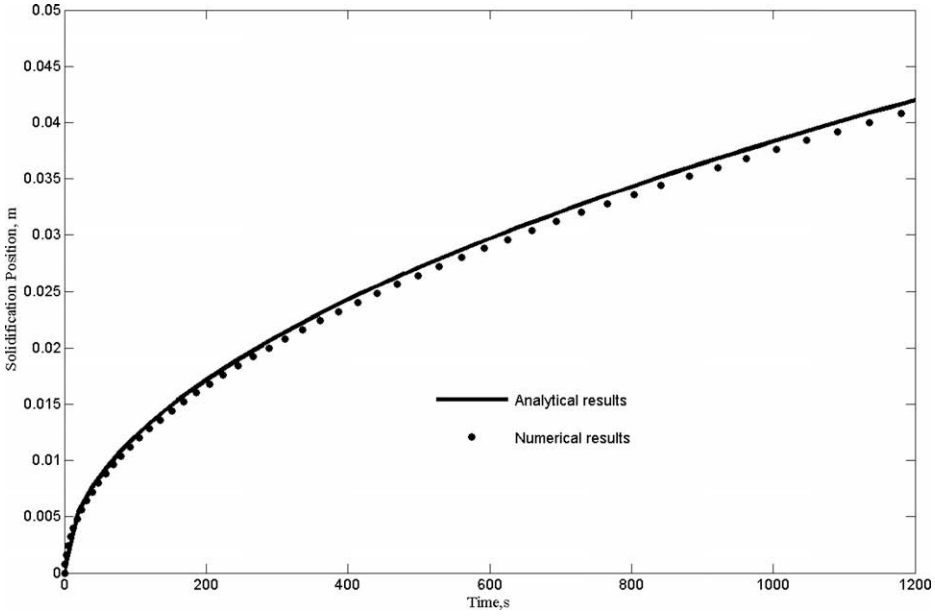


**Fig. 3.** Evolution of the advancement of solidification position with time.

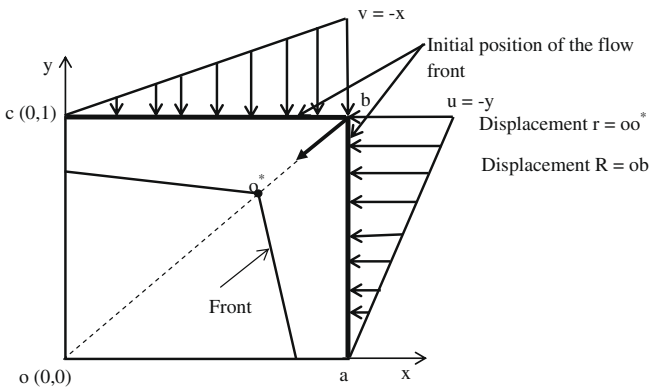


**Fig. 4.** Flow front through a square cavity within a given velocity field.

By applying the energy equation at each phase, then For solid state,

$$\frac{\partial^2 T_s}{\partial x^2} = \frac{1}{\alpha_s}\frac{\partial T_s}{\partial t} \tag{19}$$

And for liquid state

$$\frac{\partial^2 T_l}{\partial x^2} = \frac{1}{\alpha_l}\frac{\partial T_l}{\partial t} \tag{20}$$

where $\alpha_l$ and $\alpha_s$ are the thermal diffusivities for the liquid and solid phase, respectively, and they are represented as

$$\alpha_s = \frac{\lambda_s}{\rho_s C_{ps}} \quad \alpha_l = \frac{\lambda_l}{\rho_l C_{pl}} \tag{21}$$

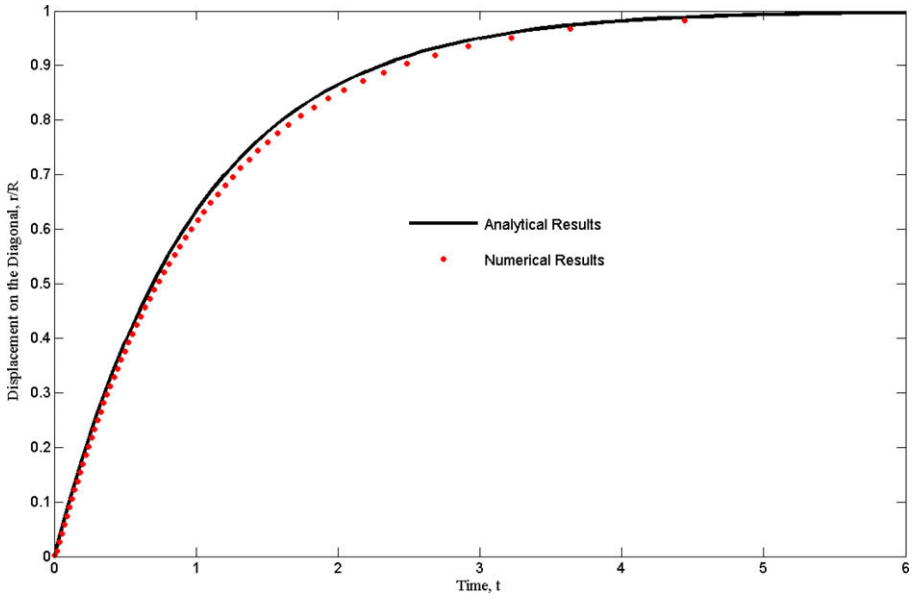


**Fig. 5.** Comparison of the numerical result with the analytical solution.

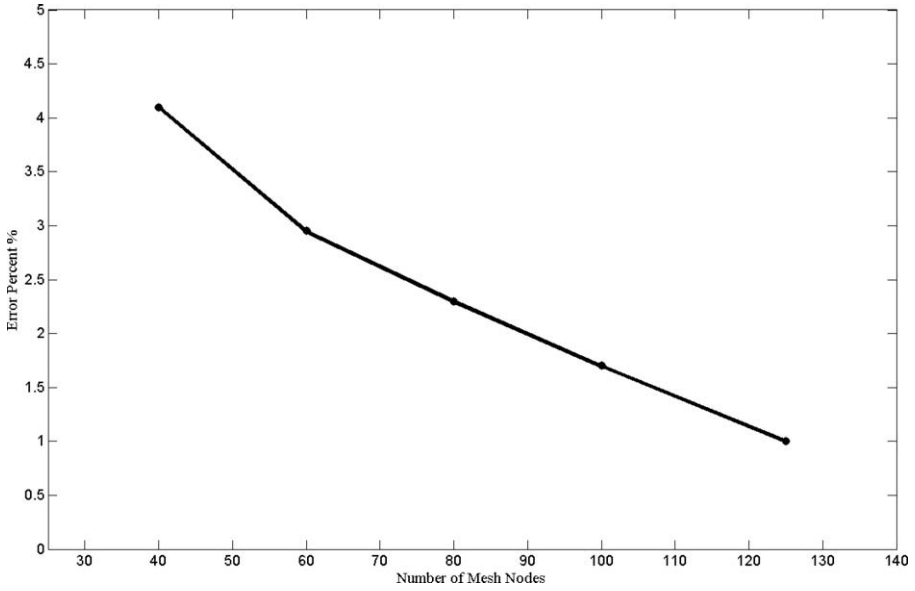


**Fig. 6.** Change of the error percent with number of mesh grid nodes (square grids).

**Table 3**
Cooling operating parameters.

| Cooling operating parameter | |
|---|---|
| Inlet temperature of the coolant fluid | 30 °C |
| Injection temperature of polymer | 220 °C |
| Melting temperature of polymer | 110 °C |
| Latent heat of polymer | 115 kJ kg$^{-1}$ K$^{-1}$ |
| Temperature of ambient air | 30 °C |
| Time of injection stage | 4.2 s |
| Time of cooling stage | 37.5 s |
| Mold opening time | 3 s |
| Diameter of the cooling channels | 8 mm |
| Total flow rate of cooling water | 1e$^{-4}$ m$^3$ s$^{-1}$ |

**Table 4**
Material properties.

| Material | Density (kg m$^{-3}$) | Specific heat (J kg$^{-1}$ K$^{-1}$) | Conductivity (W m$^{-1}$ K$^{-1}$) |
|---|---|---|---|
| Mold | 7670 | 426 | 36.5 |
| Polymer | 938 | 2280 | 0.18 |
| Cooling water | 1000 | 4185 | 0.6 |
| Air | 1.17 | 1006 | 0.0263 |

Boundary and initial conditions are:

$$T_s(x=0,t)=0 \tag{22}$$
$$T_s(x=x(t),t)=T_l(x=x(t),t)=T_f-T_{x=o}=T_f \tag{23}$$
$$T_l(x\to\infty,t)=T_o-T_{x=o}=T_o \tag{24}$$
$$T_l(x,t=0)=T_o \tag{25}$$

By the solution of the above differential equations, the following expression for the temperature distribution through the solid and liquid phase is obtained:

$$T_s(x,t)=\frac{T_f}{erf\,\xi}erf\frac{x}{2\sqrt{\alpha_s t}} \tag{26}$$
$$T_l(x,t)=T_o-\frac{T_o-T_f}{erf\,\xi\sqrt{\frac{\alpha_s}{\alpha_l}}}erfc\frac{x}{2\sqrt{\alpha_l t}} \tag{27}$$

By equalizing the above temperatures given in the interface between the two phases, then:

$$T_o-\frac{T_o-T_f}{erf\,\xi\sqrt{\frac{\alpha_s}{\alpha_l}}}erfc\frac{x(t)}{2\sqrt{\alpha_l t}}=\frac{T_f}{erf\,\xi}erf\frac{x(t)}{2\sqrt{\alpha_s t}}=T_f \tag{28}$$

This relation must be valid for each instant of time, this is possible only if $x(t)$ is proportional with $\sqrt{t}$, and this could be written as

$$x(t)=2\xi\sqrt{\alpha_s t} \tag{29}$$

where $x(t)$ is the displacement of the solid front and $\xi$ is the dimensionless equation constant and it satisfies the following transcendental equation (Feidt, 1990):

$$\frac{L\sqrt{\pi}}{C_{Ps}T_f}\xi=\frac{e^{-\xi^2}}{erf\,\xi}-\frac{\lambda_l}{\lambda_s}\sqrt{\frac{\alpha_s}{\alpha_l}}\frac{T_o-T_f}{T_f}\frac{e^{-\frac{\alpha_s}{\alpha_l}\xi^2}}{erfc\,\xi\sqrt{\frac{\alpha_s}{\alpha_l}}} \tag{30}$$

The solution of the analytical Eq. (30) for the numerical parameters and material properties shown at (Table 2) gives $\xi$ equals to 0.5825. The advancement of the solidification through $x$ direction with time in case of analytical and numerical solutions is shown in Fig. 3. (Fig. 3) shows a good agreement between the analytical and numerical solution.

*3.3.2. Filling a square cavity*

The example consists in filling a unit square cavity where a velocity field is imposed at the boundary as shown in Fig. 4 (Gao, 1999).

$$\begin{aligned} u&=-y\\ V&=-x \end{aligned} \tag{31}$$

Since the velocity is steady, the particle pathlines and the streamlines are coincident, and governed by

$$y^2=x^2+C_1 \tag{32}$$

where $C_1$ is a constant.

The magnitude of the velocity vector $|U|$ is equal to $(x^2+y^2)^{1/2}$. The initial front is assumed as straight lines *ab* and *bc*. When, the fluid fills the square cavity from the top and right sides, the

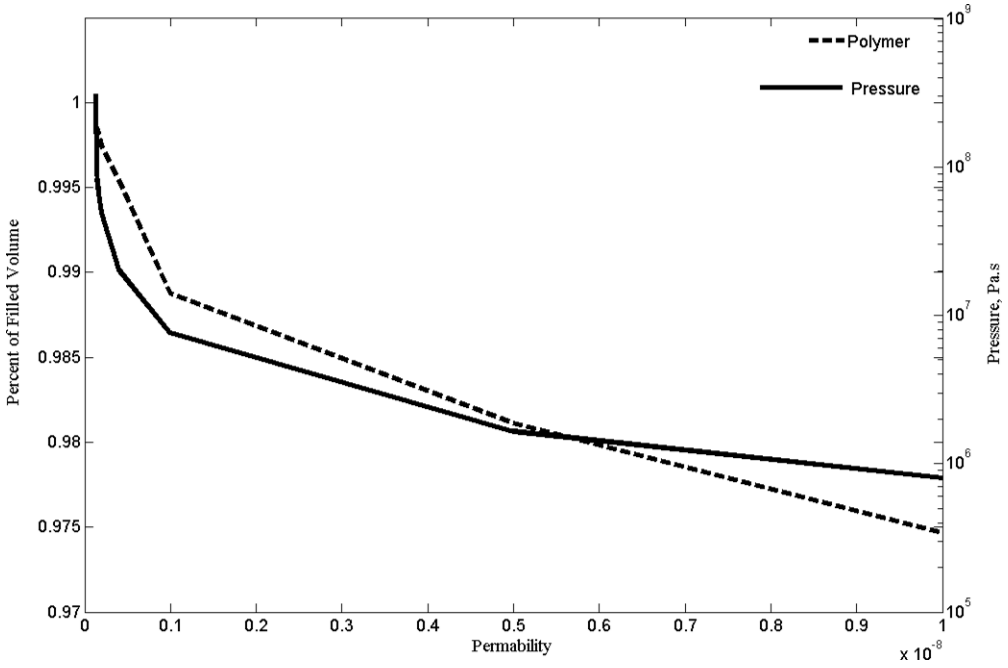


**Fig. 7.** Changing the percent volume filled - - and inlet pressure to the cavity – with changing of permeability factor.

velocity diminishes and vanishes at the origin $o$. Since the particle at the point $b$ will flow along the square diagonal.

Then the analytical solution of the non-displacement ($r/R$) versus filling time ($t$) is Gao (1999).

$$r/R = 1 - e^{-t} \tag{33}$$

where $r$ is the particle displacement $|bo^*|$ and R is the length of the diagonal $|bo|$ as shown in the (Fig 4).

In order to compare the numerical results with the analytical solution, the flow front position at the diagonal is calculated at various times. A good agreement between the numerical solution and the analytical solution is obtained during the entire filling process as shown in Fig. 5. Fig. 6 represents the mesh grid study at instant of filling time equals to 3 s. It shows that spatial convergence is obtained with second order convergence. The error percent is obtained by the following equation:

$$Error\ percent = \frac{|(r/R)_{num} - (r/R)_{th}|}{(r/R)_{th}} \tag{34}$$

The figure shows that the error increases when the number of mesh nodes decreases and the error is about 1.5% at number of mesh nodes ($100 \times 100$).

## 4. Results and discussions

A full three dimensional time-dependent injection molding analysis is carried out for a mold model with cuboids-cavity having two different thicknesses as shown in Fig. 1. The cooling of the product is carried out by using six horizontal cylindrical cooling channels. All the cooling channels have the same size and they are 8-mm diameter. The cooling operating parameters and the material properties are listed in Tables 3 and 4, respectively, (Alexandra, 2004; Qiao,

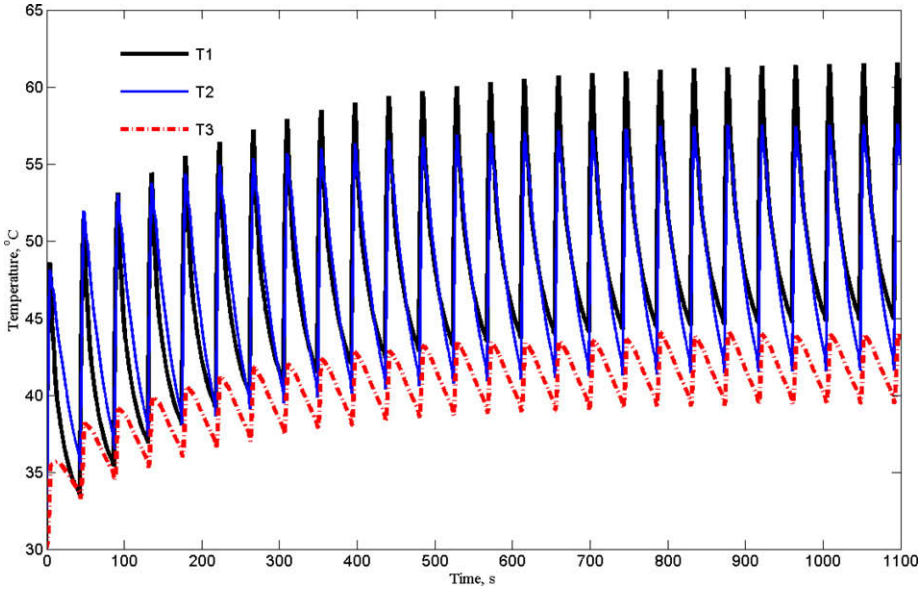


**Fig. 8.** Temperature history of the first 25 cycles for locations T1–T3 at mold wall for gate position 1.

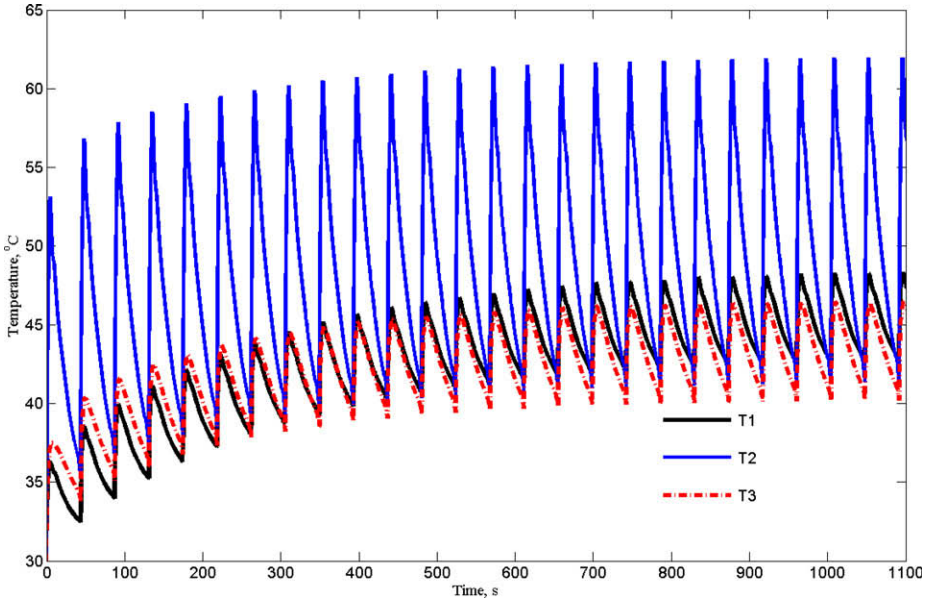


**Fig. 9.** Temperature history of the first 25 cycles for locations T1–T3 at mold wall for gate position 2.

2005) and they are considered constant during all numerical simulation except illustrated within the text.

In our numerical model, each numerical simulation consists of three main stages. Injection stage at which hot polymer is injected into the mold cavity at constant injection temperature and constant flow rate. Cooling stage where the polymer injected is cooled until the end of cooling time. The ejection stage where the cavity is assumed filled with air which is initially at ambient temperature. Three positions for the gate location are selected, normal to the small thickness (position 1), normal to the cavity surface (position 2), and normal to the large thickness of the cavity (position 3). All operating parameters are the same for the three positions. The simulation is performed for the first 35 injection molding cycles.

The mold cavity must be completely filled with hot polymer, so we assume that the air escapes from the mold cavity through a thinned layer of porous medium having the same properties of mold material with thickness of 1 mm as shown in Fig. 1. According to Eq. (15), the permeability factor $K$ determines the capability of a porous medium to let the fluid passes more or less freely through it.

According to the Darcy law (Simacek and Advani, 2004)

$$V = -\frac{K}{\mu}\nabla P \tag{35}$$

By considering the air viscosity, injection pressure, the time required withdrawing the air from the cavity that is equal to the filling time, and the total volume of the mold cavity, it is found that the value of permeability $K$ must not be less than $10^{-12}$ to completely withdraw the air from the mold cavity. Fig. 7 shows the influence of the permeability factor $K$ on the percent of filled cavity volume and the inlet pressure to the cavity. It shows that when the value $K$ increases, the filled volume of the cavity by polymer and the pressure at the cavity entrance decrease. When the value of $K$ increases, the polymer material would escape to the porous medium. Hence,

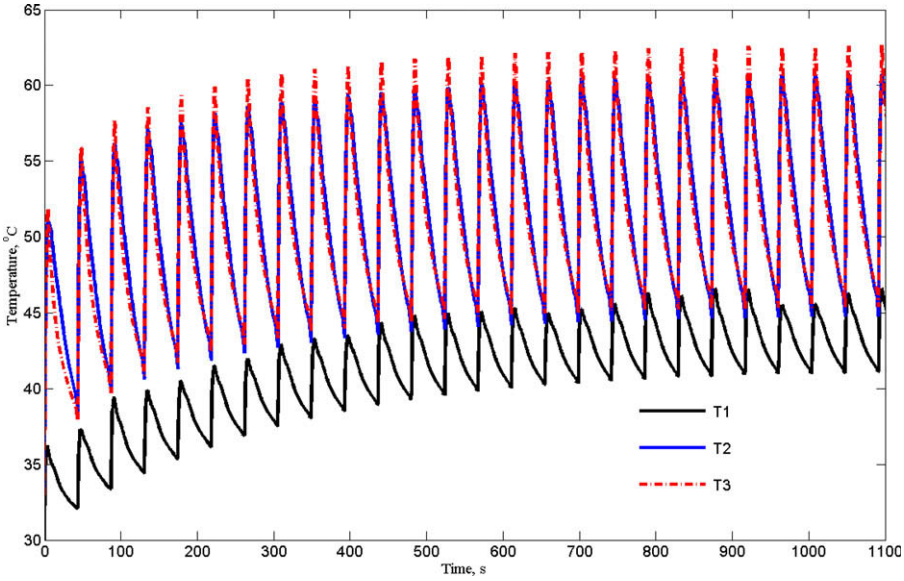


**Fig. 10.** Temperature history of the first 25 cycles for locations T1–T3 at mold wall for gate position 3.

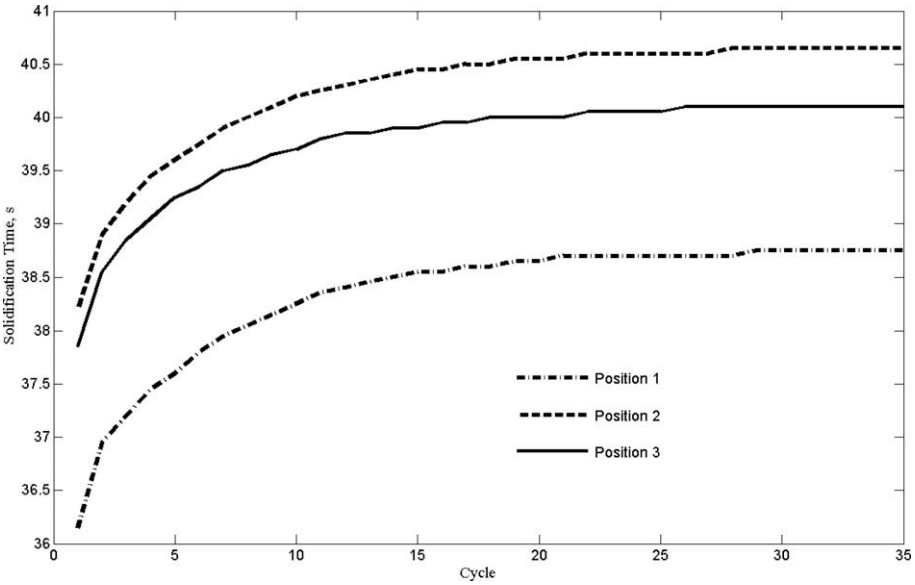


**Fig. 11.** The variation of the solidification time required for completely solidifying the product with injection molding cycle at different gate positions.

because of the volume inters the cavity is constant, the filled volume of the cavity with polymer decreases. A value of $K$ equals $10^{-10}$ m$^2$ is chosen which gives the maximum percentage of the cavity volume filled with polymer. It is also adequate for the air to escape from the mold cavity and trap the polymer inside the cavity during the filling process. Moreover, it provides at the inlet to the cavity a pressure equivalent to the pressure of the injection molding machine (25–75 MPa) (Shi et al., 2003) as shown in Fig. 7.

Gate location will affect the filling time and temperature and pressure distributions by altering the direction of the polymer flow. An improper choice of gate location can cause over packing, high shear stress, poor welds, and excessive warpage among other things. Therefore, to obtain an acceptable injection-molded part, it is necessary to search for an optimum gate location (Pandelidis and Zou, 1990).

The mold temperature is an important factor in injection molding thermoplastics and has a significant influence on the injection molding cycle and the quality of molded parts (Catic, 1979). Figs. 8–10 show the cyclic transient variations of the mold temperature with time at the mold wall for the first 25 cycles (locations T1, T2, and T3, (Fig. 1) at gate positions 1, 2 and 3, respectively. It is found that the simulated results are in good agreement with the transient characteristic of the cyclic mold temperature variations described in Qiao (2005). The figures show that the temperature fluctuation is largest near the gate position and diminishes away from that position. The figures show that the maximum amplitude of temperature fluctuation during the steady state cycle reaches about 20 °C and the minimum fluctuation is about 7 °C. The results show that the cyclic mold temperature (the variation of the mold temperature at each cycle) reaches steady state after about 20 cycles. Concerning the values of the temperature T1, T2, and T3, the positions of T1 and T3 are at the extremes sides of the mold cavity thus means they cool rapidly. For the case of the gate position 2, the temperatures at the sides T1, and T3 are smaller than T2, because

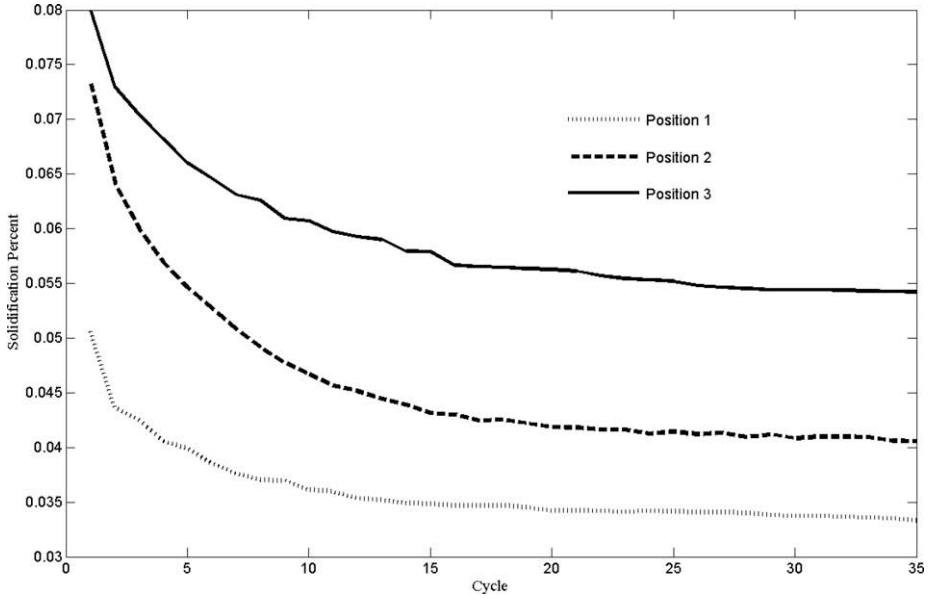


**Fig. 12.** The variation of the solidification percent of the product at the end of filling stage with injection molding cycle at different gate positions.

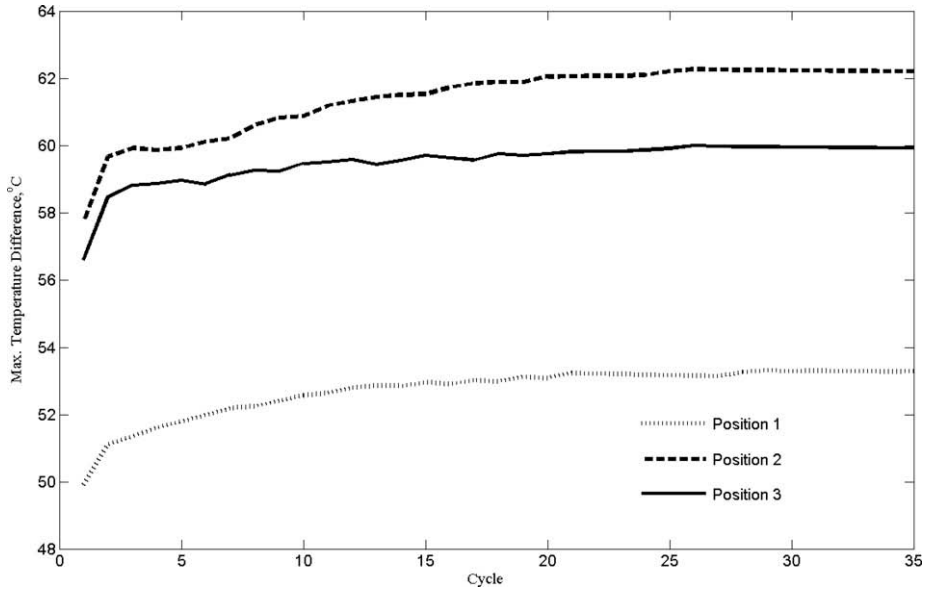


**Fig. 13.** The variation of the maximum temperature difference within the product at the end of cooling stage with injection molding cycle at different gate positions.

the polymer reaches at the sides of the mold cavity cooler and the rate of cooling at position 2 is smaller than positions 1 and 3 as shown in Fig. 9. For the other cases of gate locations, the polymer reaches to other side of the cavity cooler due to filling time, which represents 11% of the cooling time and the long path which the polymer takes through the mold cavity filling.

A reduction in the time spent on cooling the part before it is ejected, would drastically increase the production rate, and hence reduces costs. It is therefore important to understand and thereby optimize the heat transfer processes within a typical molding process efficiently. The variation of the time required to completely solidify the product at each injection molding cycle for different gate positions is shown in Fig. 11. Fig. 11 shows that the gate position 1 (normal to the small thickness of the cavity) has the minimum time required for the solidification of the product. It also shows that for steady state cycles and in case of gate position 1, the maximum time required to completely solidify the product represents 92.5% of the total time of (injection + cooling stages) and in case of gate position 2 represents 97.5%.

To completely fill the mold cavity and minimize injection pressure, we must avoid as possible the solidification of the product during the injection stage. Fig. 12 shows the variation of the solidification percent for different gate positions at the end of injection stage for each injection molding cycle. It shows that the gate position 1 has the minimum solidification percent of the product at the end of filling stage and gate position 3 has the maximum solidification percent for each injection molding cycle. It also shows that the solidification of the product during the injection stages decreases with advancing of injection molding cycles due to gradually heating of the mold material.

The final form and properties of the product depend on the temperature of the product when it exits from the mold. The maximum temperature difference (MTD) is used to express the temperature of the ejected product. This means that when the product exits from the mold with minimum MTD (MTD approaches to zero), the final shape of the product takes the required form from it. (Fig. 13) shows the variation of the maximum temperature difference inside the product at the end of cooling stage with injection molding cycle. It shows that gate position 1 has the smallest MTD and gate position 2 has the greatest MTD.

After demolding, the residual stresses (thermal and flow induced stress) will redistribute and cause the part shrinkage and warpage. Thermal induced residual stress is caused by non-uniform cooling of the molding part. Possible thermal stresses may still be introduced into the part after demolding because of further cooling to the room temperature (Wang and Young, 2005). The temperature distribution through the product at the end of cooling stage, at plane *XZ* parallel to cross section LL and for 34th injection molding cycle at gate position 1, 2 and 3 are shown in Figs. 14–16, respectively. The figures show that, the product has a minimum temperature in case of gate position 1 and a maximum temperature in case of gate position 3. They also show that, for gate position 3, the product has the maximum temperature difference between thin and thick part. From the analysis of the temperature distribution for all gate positions, it is found that the thick part has the maximum temperature which means this part requires more cooling to arrive a homogeneous temperature with the thin part. (Figs. 14 and 15) indicate that in case of gate positions 1 and 2, the temperature distribution through the product divides into two zones. Between the two zones, there is a zone of cooled temperature. These zones of the different temperature distribution and

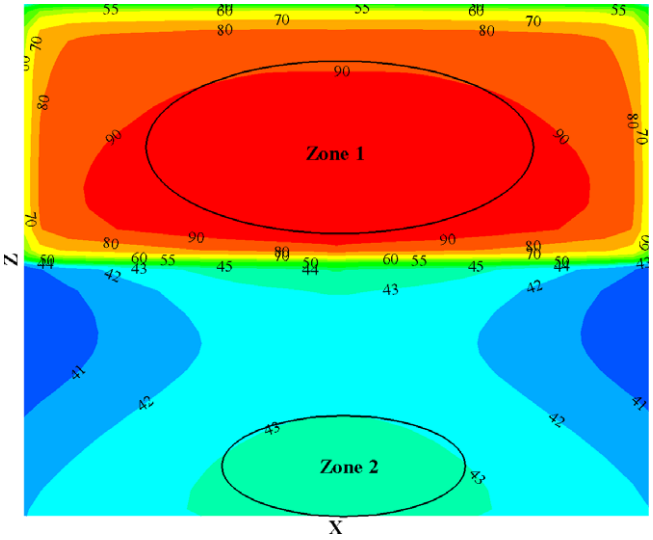


**Fig. 15.** Temperature distribution (°C) at plane *XZ* through the product at the end of cooling stage for the 34th cycle for gate position 2.

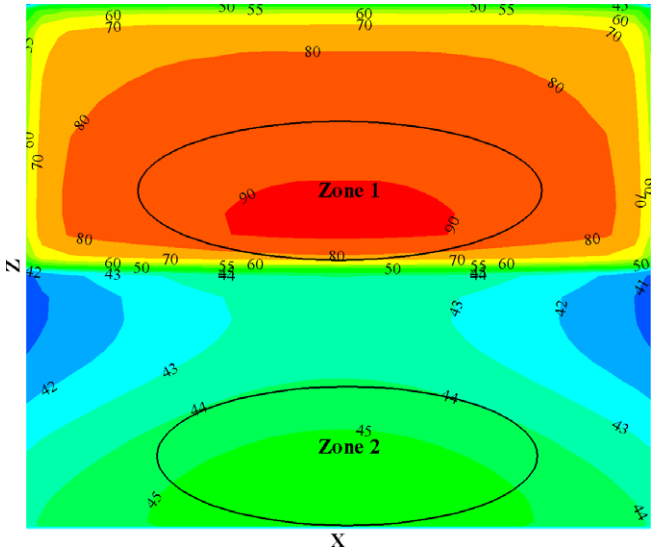


**Fig. 14.** Temperature distribution (°C) at plane *XZ* through the product at the end of cooling stage for the 34th cycle for gate position 1.

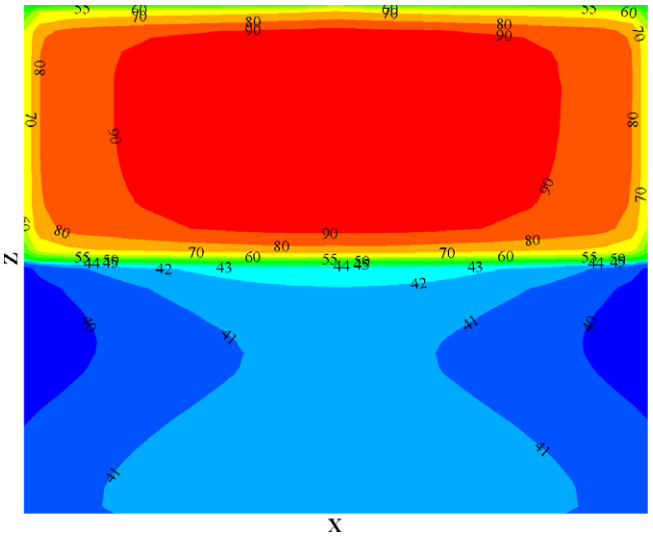


**Fig. 16.** Temperature distribution (°C) at plane *XZ* through the product at the end of cooling stage for the 34th cycle for gate position 3.

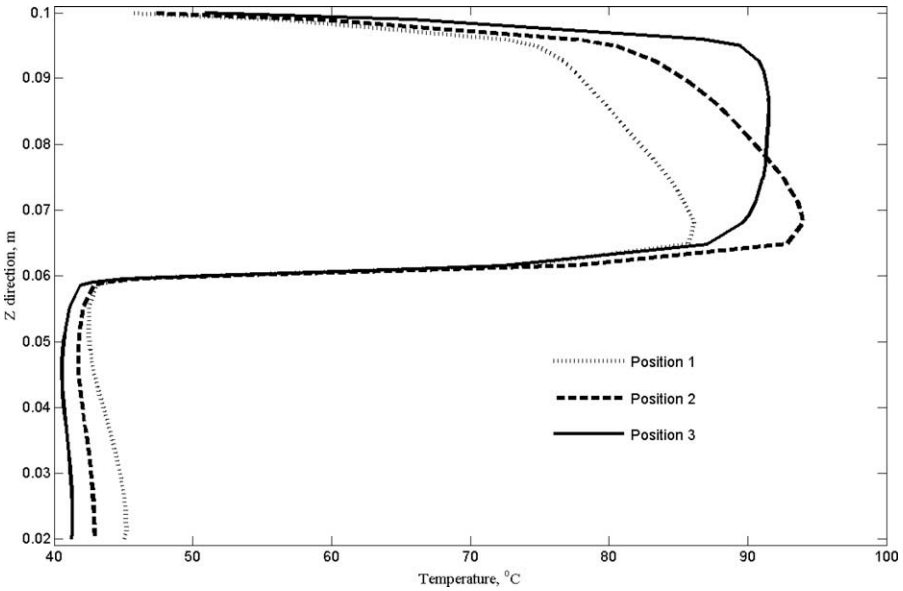


**Fig. 17.** Changing of the average temperature at *Z* direction parallel to cross section LL at different gate positions.

different cooling rates through the cooling process lead to different severe warpage and thermal residual stress in the final product which affect on the final product quality. These results are clear when comparing the average temperature inside the product at the end of the cooling stage parallel to section LL (Fig. 1) at *Z* direction as is shown in Fig. 17. (Fig. 17) shows that the variation of the average temperature inside the thick part and thin part along *Z* direction is constant for position 3 (each part shrinks at the same rate, this means the form of each part does not change after shrinkage). It also shows that the maximum difference of the temperature between the thick and thin part is about 20% of the injection temperature for all injection gate positions.

## 5. Conclusions

The effect of the injection gate position on the cooling process of injection molding is studied for polymer product having the form of cuboids with two different thicknesses. Three gate locations are assumed, normal to small thickness, normal to the surface cavity, and normal to the large thickness of the cavity. A finite volume method is used for the solution of the mathematical model. The validation of the numerical model shows a good agreement between the numerical and analytical solution. The results indicate that for gate position normal to the small thickness of the cavity, the injection molding process has the minimum time required to solidify the product, the minimum solidification percent during the filling stage and the minimum temperature difference through the product after demolding. They also show that the gate position has a great effect on the temperature distribution of the injected molded product. With this thermal analysis of the gate position effect and a supplementary analysis on his effect on the residual stresses and warpage of the final product and the stability of injection molding machine, an optimum gate location could be determined.

## References

Alexandra, R. Luısa, 2004. Viscoelastic compressible flow and applications in 3D injection molding simulation. Ph.D. Thesis, L'école National Superiere des Mines des Paris, France.

Angot, Ph., 1989. Contribution à l'étude des transferts thermiques dans les systèmes complexes. Application aux composants électroniques. Ph.D. Thesis, Bordeaux 1 University, Bordeaux, France.

Arquis, E., Caltagirone, J.P., 1984. Sur les conditions hydrodynamiques au voisinage d'une interface milieu fluide milieu poreux: application à la convection naturelle. C. R. Academy of Sciences Séries IIb, France 299, 1–4.

Catic, Igor J., 1979. Cavity temperature – an important parameter in the injection molding process. Polymer Engineering and Science 19 (October), 893–899.

Chiang, H.H., Hieber, C.A., Wang, K.K., 1991. A unified simulation of the filling and post filling stages in injection molding part I: formulation. Polymer Engineering and Science 31, 116–124.

Feidt, M., 1990. Transfert de chaleur et de matière avec changement de phase. Pont-A-Mousson, Juillet, France.

Gao, D.M., 1999. A three dimensional hybrid finite element-volume tracking model for mould filling in casting process. International Journal for Numerical Methods in Fluids 29, 877–895.

Haddad, Header, Masood, S.H., Saifullah, B.M., 2008. Gate location and its effects on product quality in injection molding. Advanced Material Research 32, 181–184.

Huang, Xiao Yan, Li, De-Qun, Xu, Qiang, 2008. Gate location optimization in injection molding based on empirical search method. Materials Science Forum 575–578, 55–62.

Kang, Moon Koo, Jung, Jae Joon, Lee, Woo, 2000. Analysis of resin transfer moulding process with controlled multiple gates resin injection. Composites: Part A 31, 407–422.

Khadra, K., 1994. Méthodes adaptatives de raffinement local multi grille, applications aux équations de Navier-Stokes et de l'énergie. Ph.D. Thesis, Bordeaux 1 University, Bordeaux, France.

Kima, H.S., Sonb, J.S., Imc, Y.T., 2003. Gate location design in injection molding of an automobile junction box with integral hinges. Journal of Materials Processing Technology 140, 110–115.

Le, Bot, 2003. Impact et solidification de gouttes métalliques sur un substrat solide. Ph.D. Thesis, Bordeaux 1 University, Bordeaux, France.

Lee, B.H., Kim, B.H., 1996. Automated selection of gate location based on desired quality of injection molded part. Polymer–Plastics Technology and Engineering 35, 253–269.

Li, Ji quan, Li, De-qun, Guo, Zhi-ying, Lv, Hai-yuan, 2007. Single gate optimization for plastic injection mold. Journal of Zhejiang University Science A 8, 1077–1083.

Min, B.H., 2003. A study on quality monitoring of injection-molded parts. Journal of Materials Processing Technology 136, 1–6.

Pandelidis, Ioannis, Zou, Qin, 1990. Optimization of injection molding design part I: gate location optimization. Polymer Engineering and Science 30, 873–882.

Qiao, H., 2005. Transient mould cooling analysis using the BEM with the time-dependent fundamental solution. International Communication in Heat and Mass Transfer 32, 315–322.

Shi, F., Lou, Z.L., Lu, J.G., Zhang, Y.Q., 2003. Optimisation of plastic Injection moulding process with soft computing. International Journal of Advanced Manufacturing Technology 21, 656–661.

Simacek, Pavel, Advani, Suresh G., 2004. Gate elements at injection locations in numerical simulations of flow through porous media: application to mold filling. International Journal for Numerical Methods in Engineering 61, 1501–1519.

Tang, S.H., Kong, Y.M., Sapuan, S.M., 2006. Design and thermal analysis of plastic injection mold. Journal of Materials Processing Technology 171, 259–267.

Vincents, S., 1999. Modélisation d'écoulements incompressibles des fluides non miscibles. Ph.D. Thesis, Bordeaux 1 University, Bordeaux, France.
Vincent, S., Arquis, E., 2000. Numerical modeling of cooling and solidification of molten particles impacting a solid substrate. Société Française de Thermique 8, 371–375.
Vincent, S., Caltagirone, J.P., 2000. A one-cell local multi-grid method for solving unsteady incompressible multiphase flows. Journal of Computational Physics 163, 172–215.
Wang, Tong-Hong, Young, Wen-Bin, 2005. Study on residual stresses of thin-walled injection molding. European Polymer Journal 41, 2511–2517.
Zhai, M., Lam, L.C., Au, C.K., 2005. Algorithms for two gate optimization in injection molding. International Polymer Processing 20, 14–18.
Zhai, M., Lam, L.C., Au, C.K., 2006. Runner sizing and weld line positioning for plastics injection molding with multiple gates. Engineering with Computers 21, 218–224.